Expanded View Figures

Figure EV1. Knockdown of *dpr12* results in regrowth phenotype and description of *Dpr12* alleles used in the study, related to Fig 1.

A Left: Graphs depicting the normalized RNA expression levels of selected Dprs in WT γ-KCs (black), and in γ-KCs expressing EcR^{DN} (green) or UNF-RNAi (blue). $^*P < 0.05$; Error bars indicate SEM; units on the y-axis are arbitrary. Right: Confocal z-projections of adult γ-KCs expressing RNAi transgenes as indicated labeled with membrane-bound GFP (mCD8-GFP; CD8) driven by the γ-specific Gal4 driver R71G10-Gal4 (γ-Gal4). Note that while R71G10 is consistently expressed in γ-KCs, it is also expressed in α/β-KCs in a stochastic manner.

B A schematic representation of the *Dpr12* locus showing introns (black line) and coding and non-coding exons (red and gray, respectively). The location of *Dpr12* gRNA (arrow), $dpr12^{\Delta 50\text{-}81}$ mutation (arrow), *dpr12* $RNAi^{JF03210}$ (black lines connected with dashed lines), and $MiMIC^{MI01695}$ (arrowhead) is indicated. SA and SD are splice acceptor and donor sites, respectively. Recombination-mediated cassette exchange was used to transform $Dpr12^{MI01695}$ into $Dpr12^{GFSTF}$.

C A schematic representation of Dpr12 protein variants. Signal peptide (SP), Immunoglobulin (Ig), transmembrane (TM), and GPI anchor (GPI).

D Ranking of regrowth: Confocal z-projections of adult γ-KCs labeled with membrane-bound GFP (mCD8-GFP; CD8) driven by the γ-specific Gal4 driver GMR71G10-Gal4 (γ-Gal4). Representative images of the regrowth defect severity (1 = strong, 2 = intermediate, 3 = weak, 4 = WT) described in Fig 1O. The arrowhead demarcates an unusually short β-lobe; morphologically abnormal β-lobes (either short, thin or absent) appear in approximately 40% of either *dpr12* or *DIP-δ* homozygous mutant brains. Since β-lobe morphology is rescued by overexpressing a UAS-Dpr12 transgene within γKCs, it is most likely a non-cell-autonomous defect, which is beyond the scope of this study. Asterisk demarcates the distal tip of the γ-lobe. Green is CD8-GFP; magenta is FasII staining. Scale bar is 20 μm.

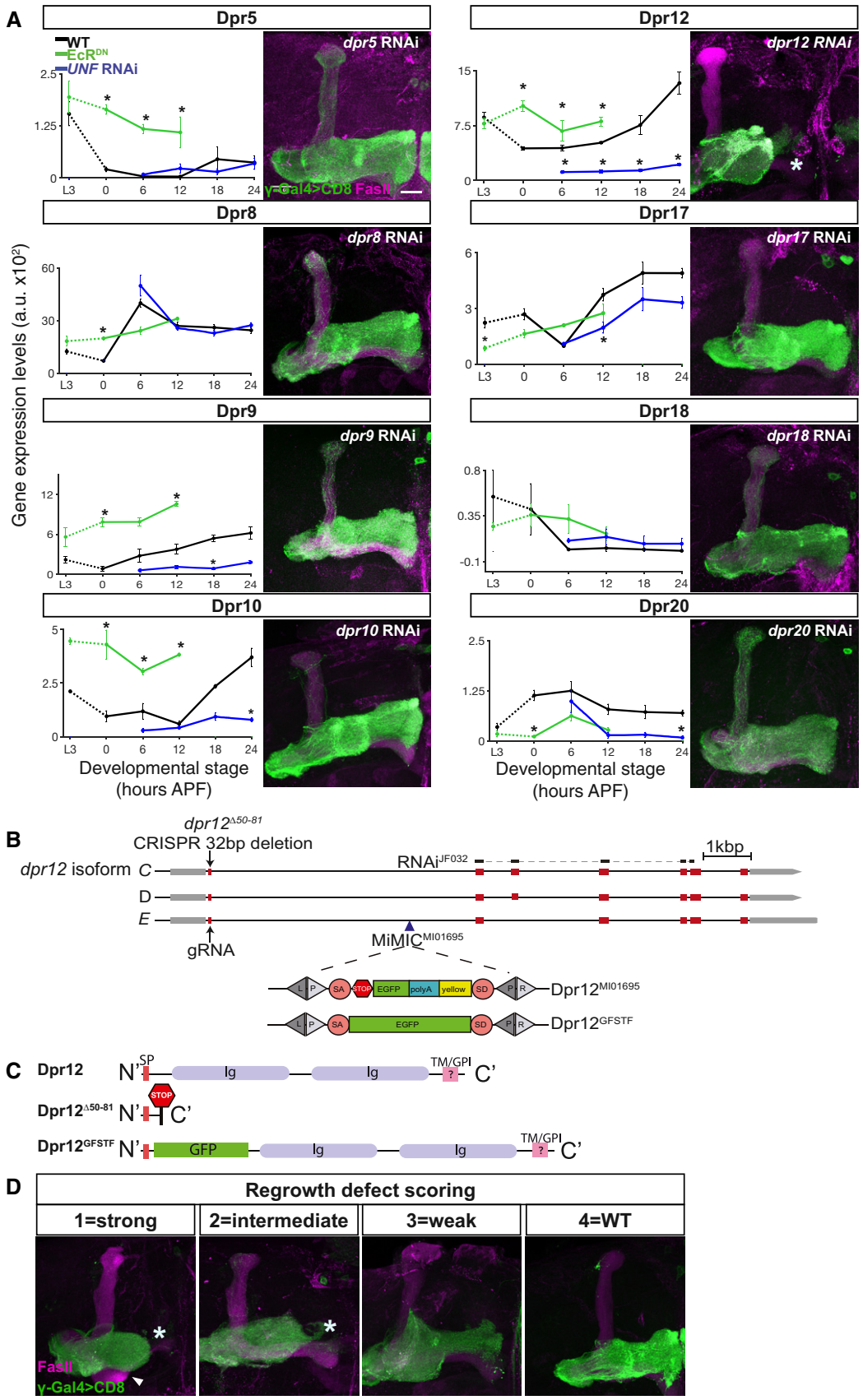
A
Dpr5
WT
EcR^DN
UNF RNAi
dpr5 RNAi
γ-Gal4>CD8 FasII
Dpr12
dpr12 RNAi
Dpr8
dpr8 RNAi
Dpr17
dpr17 RNAi
Dpr9
dpr9 RNAi
Dpr18
dpr18 RNAi
Dpr10
dpr10 RNAi
Dpr20
dpr20 RNAi
Gene expression levels (a.u. x10²)
Developmental stage (hours APF)
B
dpr12Δ50-81
CRISPR 32bp deletion
dpr12 isoform C
D
E
gRNA
RNAi JF032
1kbp
MiMIC MI01695
Dpr12MI01695
Dpr12GFSTF
EGFP
polyA
yellow
C
Dpr12
Dpr12Δ50-81
Dpr12GFSTF
SP
Ig
TM/GPI
GFP
STOP
D
Regrowth defect scoring
1=strong
2=intermediate
3=weak
4=WT
FasII
γ-Gal4>CD8

Figure EV1.

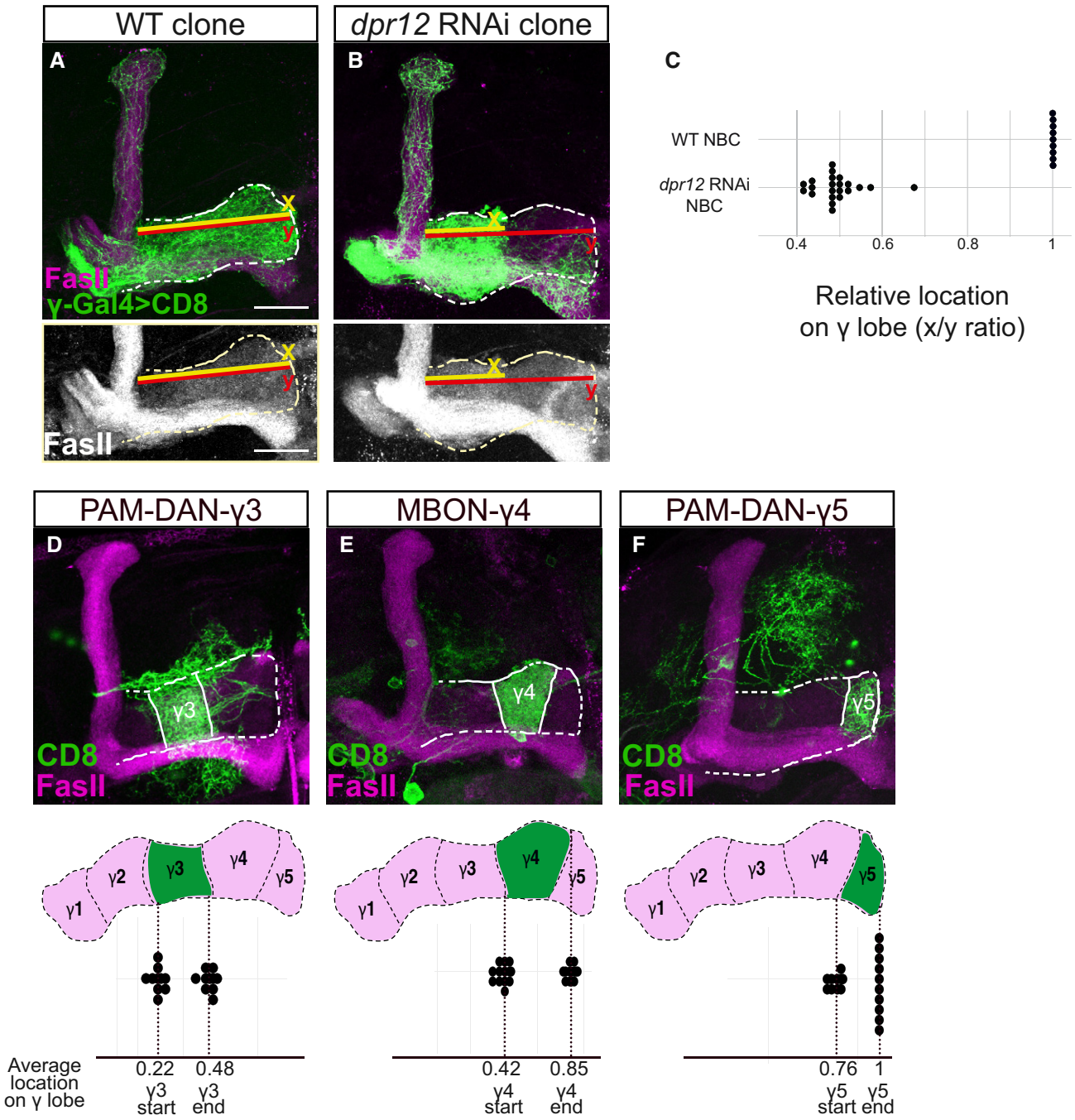

Figure EV2. Measurements of γ-axon outgrowth, related to Fig 2.

A, B Confocal z-projections of WT (A) and *dpr12* RNAi (B) MARCM neuroblast clones (NBC) labeled with membrane-bound GFP (mCD8-GFP; CD8) driven by the γ-specific Gal4 driver GMR71G10-Gal4 (γ-Gal4). y (red) represents the length of the entire γ-lobe as indicated; x (yellow) represents the extent of clonal γ-axon outgrowth.

C Measurements of the x/y ration as depicted in (A, B). While WT NBC always extends up to the end of the lobe, *dpr12* RNAi NBC stops at about midway (x/y ratio of 0.48 ± 0.05).

D–F Top: Confocal z-projections of PAM-DAN-γ3 (D, MB441B), MBON-γ4 > γ1γ2 (E, R18H09), and PAM-DAN-γ5 (F, R48H11) Gal4s driving the expression of mCD8-GFP (CD8). Bottom: start and end of the indicated zone is superimposed on a schematic representation of the adult γ lobe compartments. (D) γ3 zone begins at x/y ratio of 0.22 ± 0.03 and ends at 0.48 ± 0.03. (E) γ4 zone begins at x/y ratio of 0.42 ± 0.04 and ends at 0.85 ± 0.03. (F) γ5 zone begins at x/y ratio of 0.76 ± 0.03 and ends at a mean ratio of 1. Green is CD8-GFP; magenta and white represent FasII. Scale bar is 20 μm.

Figure EV3. Description of *DIP-δ* alleles used in the study and additional *DIP-δ* perturbation phenotypes, related to Fig 4.

A A schematic representation of the *DIP-δ* locus showing introns (black line) and coding and non-coding exons (red and gray, respectively). The location of *DIP-δ* gRNA, *DIP-δ*$^{1\text{-}119}$ mutation, *DIP-δ* RNAi, and MiMIC^{MI08287} is indicated. SA and SD are splice acceptor and donor sites, respectively. Recombination-mediated cassette exchange was used to transform DIP-δ^{MI08287} into DIP-δ^{GFSTF} and DIP-δ$^{T2A\text{-}Gal4}$.

B A schematic description of DIP-δ protein variants. Signal peptide (SP), Immunoglobulin (Ig), and GPI anchor (GPI).

C–E Confocal z-projections of DIP-δ transheterozygotes (DIP-δ$^{T2A\text{-}Gal4/1\text{-}119}$) at L3 (C; n = 20/20) and adult (D; n = 12/12, E; n = 22/23), in which γ neurons were marked by expressing membrane-bound tandem tomato (mtdT-HA) driven by the γ-specific QF2 driver GMR71G10-QF2 (γ-QF2). In DIP-δ transheterozygotes, as in homozygous mutants (see Fig 4), γ-KCs do not extend into the distal end of the lobe. Expression of DIP-δ in DIP-δ^{+} cells (E) rescues the growth defect present in DIP-δ$^{T2A\text{-}Gal4/1\text{-}119}$ brains. Green and white represent mtdT-HA; magenta represents FasII staining.

F–I Confocal z-projections of brains expressing UAS-Cas9 alone (F, H) or together with *DIP-δ*-gRNA (G, I). *DIP-δ* knockout by tsCRISPR in all postmitotic neurons (G; n = 22/24) resulted in a defect in γ4/5 innervation by γ-axons, while *DIP-δ* knockout by tsCRISPR in γ-KCs (I; n = 28/28) did not affect γ-axon regrowth. Expression of Cas9 alone (F, n = 10/10; H, n = 14/14) did not affect γ-axon regrowth. White represents FasII staining.

Data information: Scale bar is 20 μm.

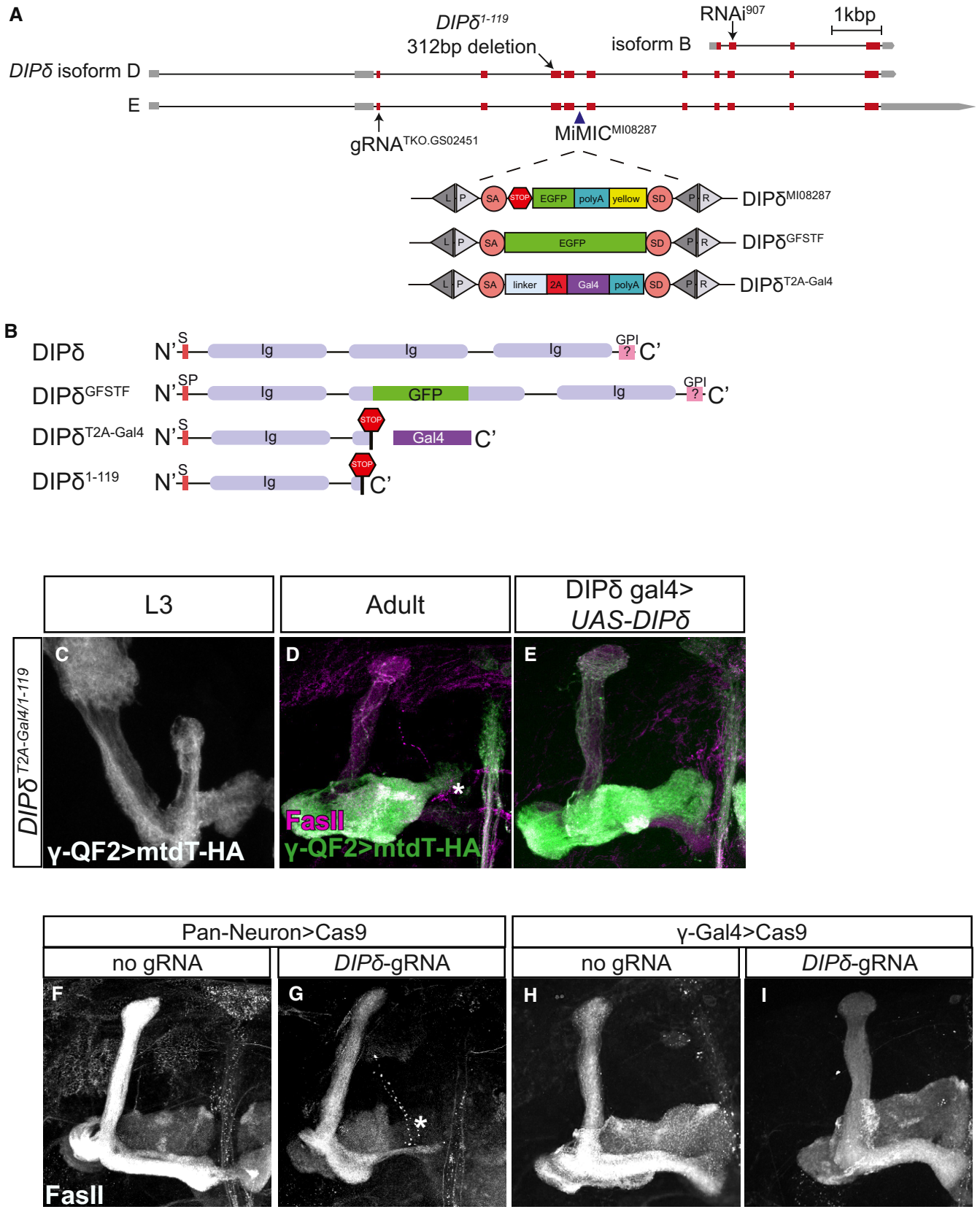

Figure EV3.

Figure EV4. Characterization of PAM-DAN and DIP-δ Gal4s, related to Fig 5.

A–C Confocal z-projections of the cell body region of the PAM-DAN cluster demonstrating the expression of membrane-bound tandem tomato (CD4-tdT; CD4) driven by *DIP-δ$^{T2A\text{-}Gal4}$* (DIP-δ-Gal4) in addition to GFP driven by the PAM-DAN specific QF2 driver GMR58E02-QF2 (PAM-QF2). The PAM-QF2 driver is not expressed at 24 h APF (A, $n = 12$), starts to be expressed at 48 h APF (B, $n = 10$) and fully expressed and localized with DIP-δ-Gal4 in adult (C, $n = 14$).

D–F Confocal z-projections of heterozygous brains (DIP-δ$^{+/T2A\text{-}Gal4}$) in which DIP-δ positive neurons were labeled by membrane-bound GFP (mCD8-GFP; CD8) driven by DIP-δ-Gal4. γ-KCs were marked by expressing membrane-bound tandem tomato (mtdT-HA) driven by the γ-specific QF2 driver GMR71G10-QF2 (γ-QF2). Bottom: High magnification images as demarcated by dashed boxes in top panels, of sub-z-projections restricted to slices that contain the γ-lobe.

Data information: Dashed outline demarcates γ-lobe as depicted by FasII staining. γ4/5 zones are indicated in adult. (D), $n = 20$; (E), $n = 16$; (F), $n = 26$. Scale bar is 20 μm.

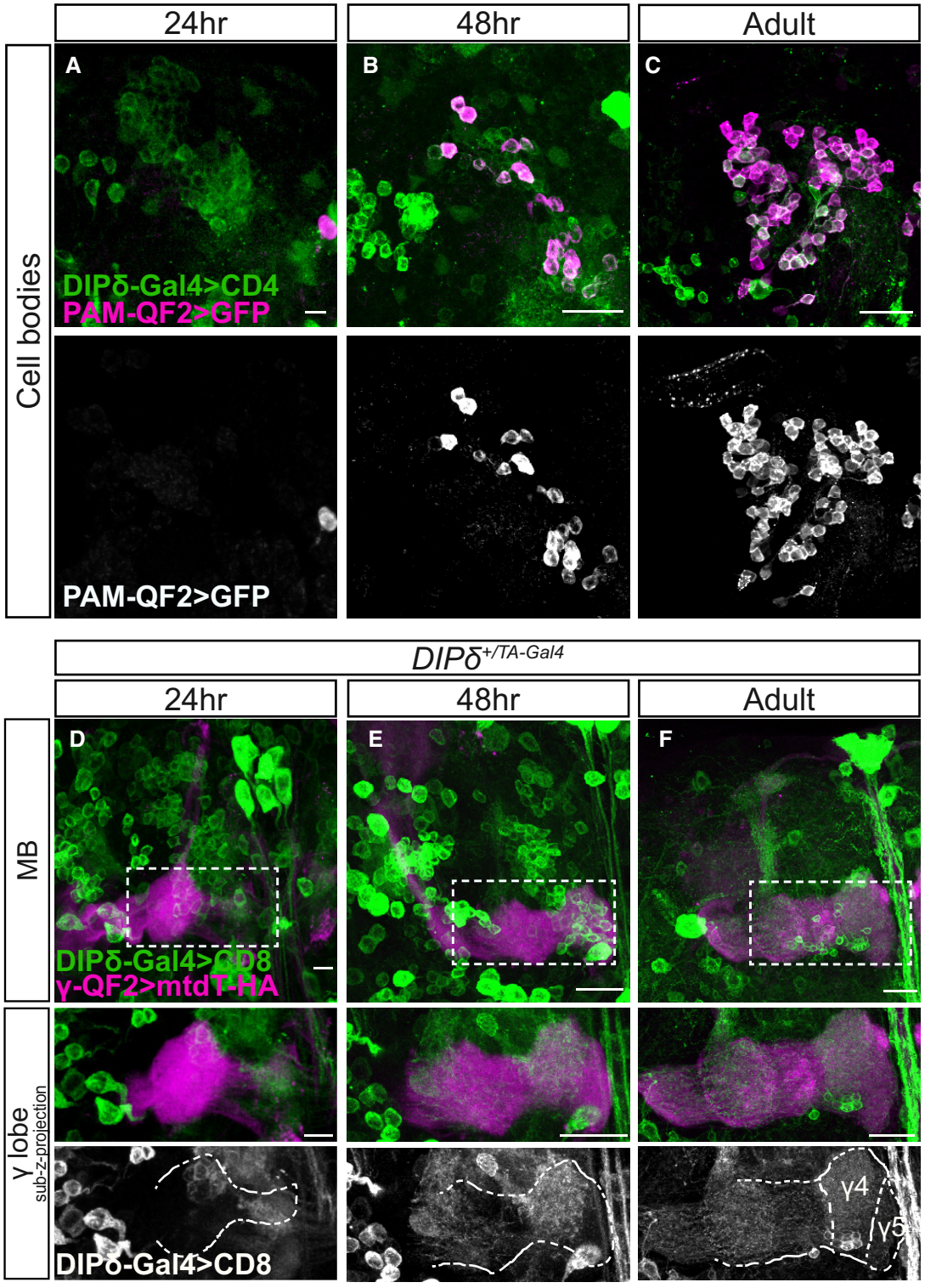

Figure EV4.

Figure EV5. Phenotypic analysis of PAM-DAN and MBON innervation of the MB γ-lobe in Dpr12 mutant brains, related to Fig 7.

A–I (A, B, D, E, G, H) Left: Detailed analysis of the confocal z-projections of *dpr12* heterozygous or homozygous mutant brains that are presented in Fig 7A–F, which express membrane-bound GFP (CD8) driven by: (A-B) R10G03-Gal4 is used to label PAM-DANs innervating the γ4 compartment (PAM-DAN-γ4); (D-E) R48H11-Gal4 is used to label PAM-DANs innervating the γ5 compartment (PAM-DAN-γ5); (G-H) R18H09-Gal4 is used to label the MBONγ4 > γ1γ2 which innervates the γ4 zone (MBON-γ4). Right: YZ projections along the indicated lines in γ3 (orange) and γ4 or γ5 (blue) compartments. (C, F, I) Top: Cell body numbers of the indicated neurons in *dpr12* heterozygous and homozygous brains. Bottom: Summary of innervation destinations. Unknown means stereotypic projections to unidentifiable domains.

Data information: Green is CD8-GFP, magenta is FasII, and grayscale single channels are shown as indicated. Asterisks mark missing innervation and arrows mark innervations outside the γ lobe. Scale bar is 20 μm in (A-B, D-E, G-H) and 10 μm in (A'-B',D'-E',G'-H').

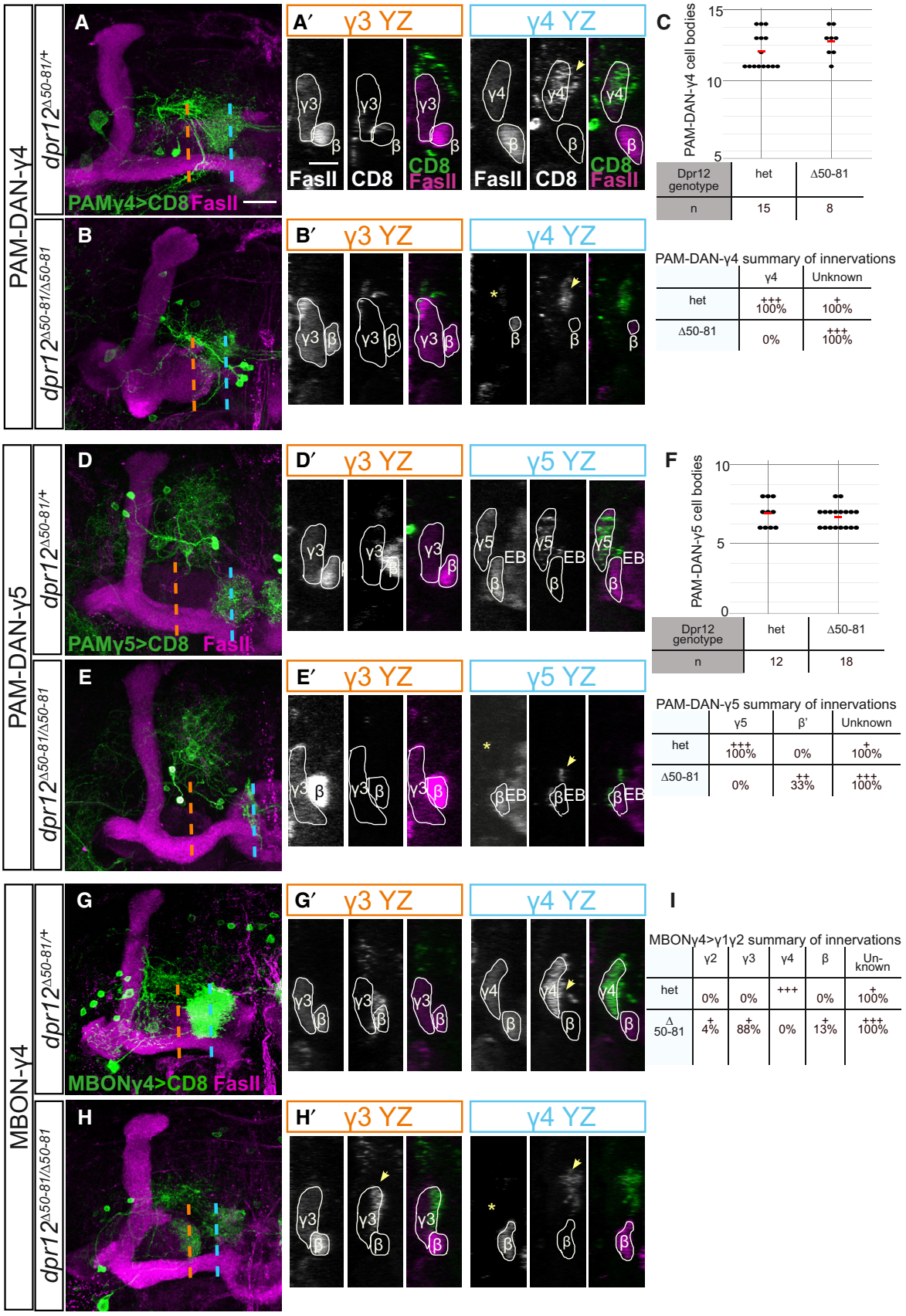

Figure EV5.

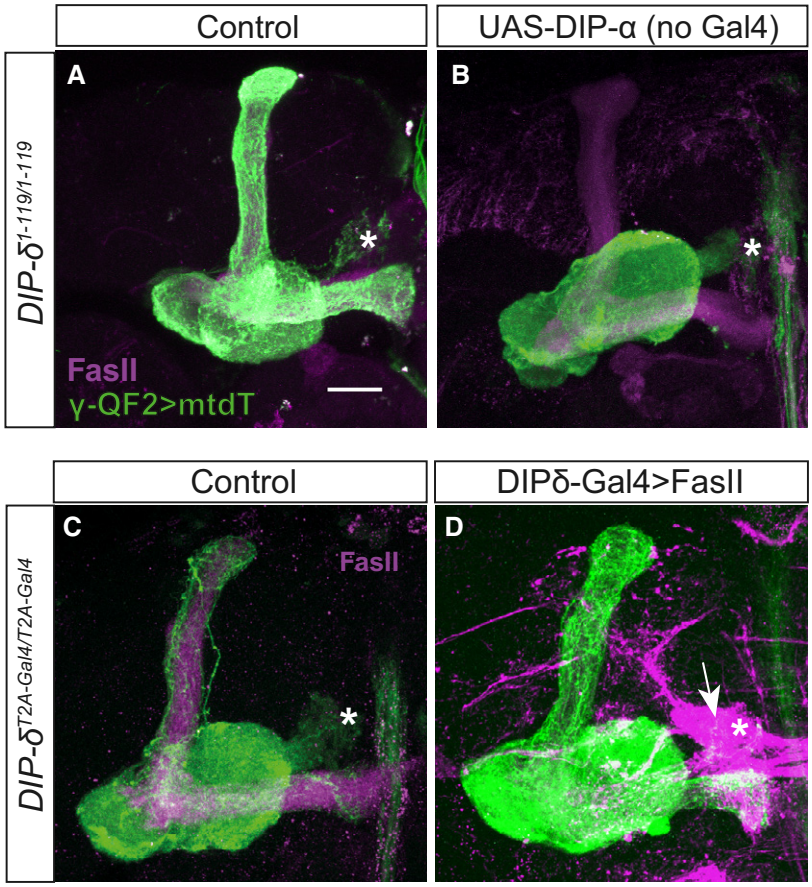

Figure EV6. UAS-DIP-α function is Gal4-dependent; FasII overexpression fails to suppress the *DIP-δ* mutant phenotype, related to Fig 8.

A, B Confocal z-projections of *DIP-δ*$^{1-119}$ homozygous mutant brains, in which γ-KCs are labeled by membrane-bound tandem tomato (mtdT-HA; green) driven by R71G10-QF2 (γ-QF2), that either contain (B) or do not contain (A) a UAS-DIP-α transgene.

C, D Confocal z-projections of *DIP-δ*$^{T2A\text{-}Gal4/T2A\text{-}Gal4}$ homozygous mutant brains, in which γ-KCs are labeled by mtdT-HA (green) driven by γ-QF2, that either express (D) or do not express (C) a UAS-FasII transgene driven by DIP-δ-Gal4.

Data information: Magenta is FasII; arrow in (D) indicates FasII accumulation in DIP-δ^{+} PAM-DANs. Asterisks mark the distal edge of the lobe. Scale bar is 20 μm.